5-21-2004

Impacts of a Recurrent Resuspension Event and Variable Phytoplankton Community Composition On Remote Sensing Reflectance

Trisha Bergmann
University of Maine

Gary Fahnenstiel
Great Lakes Environmental Research Laboratory

Steven Lohrenz
University of Southern Mississippi

David Millie
Florida Marine Research Institute

Oscar Schofield
Rutgers University

Impacts of a recurrent resuspension event and variable phytoplankton community composition on remote sensing reflectance

Trisha Bergmann,[1] Gary Fahnenstiel,[2] Steven Lohrenz,[3] David Millie,[4] and Oscar Schofield[5]

Received 30 July 2002; revised 1 July 2003; accepted 9 October 2003; published 21 May 2004.

[1] In order to characterize the impact of turbidity plumes on optical and biological dynamics, a suite of environmental parameters were measured in southern Lake Michigan during the springtime recurrent sediment plume. In-water measurements of inherent optical properties (IOPs) were entered into the Hydrolight 4.2 radiative transfer model and the output was compared with measured apparent optical properties (AOPs) across a wide range of optical conditions. Hydrolight output and measured underwater light fields were then used to clarify the effects of the sediment plume on primary production, phytoplankton community composition, and nearshore remote sensing ocean color algorithms. Our results show that the sediment plume had a negligible effect on the spectral light environment and phytoplankton physiology. The plume did not significantly alter the spectral quality of available light and did not lead to light limited phytoplankton populations compared to non-plume conditions. Further, the suspended sediment in the plume did not seriously impact the performance of ocean color algorithms. We evaluated several currently employed chlorophyll algorithms and demonstrated that the main factor compromising the efficacy of these algorithms was the composition of phytoplankton populations. As phycobilin-containing algae became the dominant species, chlorophyll algorithms that use traditional blue/green reflectance ratios were compromised due to the high absorption of green light by phycobilin pigments. This is a notable difficulty in coastal areas, which have highly variable phytoplankton composition and are often dominated by sharp fronts of phycobilin and non-phycobilin containing algae. *INDEX TERMS:* 4847 Oceanography: Biological and Chemical: Optics; 4275 Oceanography: General: Remote sensing and electromagnetic processes (0689); 4855 Oceanography: Biological and Chemical: Plankton; 4239 Oceanography: General: Limnology; *KEYWORDS:* remote sensing, phytoplankton, coastal optics

Citation: Bergmann, T., G. Fahnenstiel, S. Lohrenz, D. Millie, and O. Schofield (2004), Impacts of a recurrent resuspension event and variable phytoplankton community composition on remote sensing reflectance, *J. Geophys. Res.*, *109*, C10S15, doi:10.1029/2002JC001575.

1. Introduction

[2] The main circulation patterns in Lake Michigan are primarily wind driven. This is an energetic and dynamic environment, and it is often seriously affected by short-term episodic events. In the Great Lakes, episodic events are most frequent in the late winter/early spring when high winds and storms are prevalent and thermal stratification is low [*Lee and Hawley*, 1998; *Lou et al.*, 2000; *Beletsky and Schwab*, 2001]. These events have been hypothesized to play a disproportionately large role in structuring physical and biological systems, but investigating their importance is difficult given the limitations of traditional sampling techniques.

[3] One annual event that occurs in southern Lake Michigan each spring is a recurrent turbidity plume that extends up to 200 km alongshore [*Mortimer*, 1988]. Spring in Lake Michigan is marked by frequent, highly energetic storms, turbulent shoreline erosion, and high river runoff. These forces lead to significant resuspension of particles, which are then transported to the southern basin of the lake. The erosive forces in Lake Michigan are episodic in nature, and for many biogeochemically important materials this resuspension and transport of sediments in the Southern Basin is greater than external inputs from rivers [*Eadie et al.*, 1984; *Hawley*, 1991; *Eadie et al.*, 1996]. Particles resuspended during the plume event may comprise up to 25% of the total transport of sediment to the southern part of the Lake [*Eadie et al.*, 1996; *Lou et al.*, 2000]. This resuspension and transport of concentrated sediment loads is coincident with the spring phytoplankton bloom [*Mortimer*, 1988]. The

[1]School of Marine Sciences, University of Maine, Orono, Maine, USA.
[2]Great Lakes Environmental Research Laboratory, NOAA, Muskegon, Michigan, USA.
[3]Department of Marine Science, University of Southern Mississippi, Stennis Space Center, Mississippi, USA.
[4]Florida Marine Research Institute, FWCC and Florida Institute of Oceanography, Saint Petersburg, Florida, USA.
[5]Coastal Ocean Observation Lab, Institute of Marine and Coastal Sciences, Rutgers University, New Brunswick, New Jersey, USA.

0148-0227/04/2002JC001575

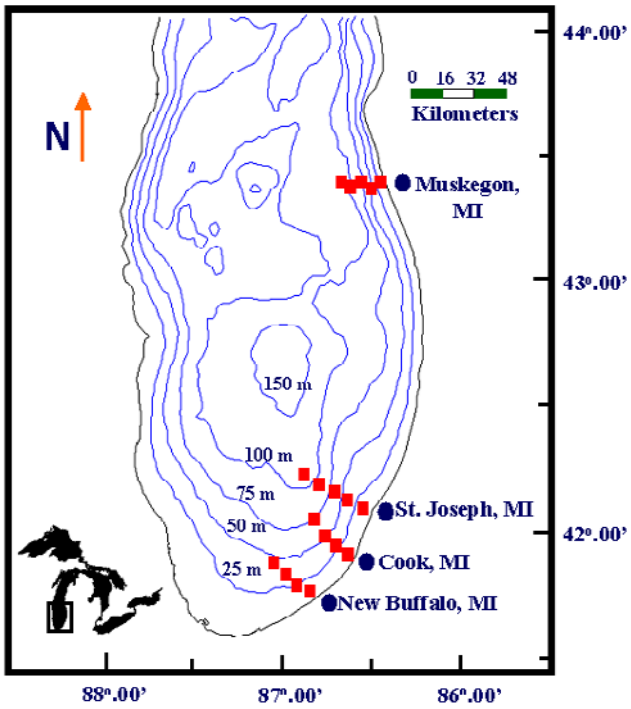

Figure 1. Sampling locations in southeastern Lake Michigan occupied in 1998–2000.

spring bloom is a crucial time for the ecology of Lake Michigan as it may contribute up to 50% of the total annual primary production in the Lake and is a major source of carbon to higher trophic levels [*Fahnenstiel and Scavia*, 1987]. The physical processes associated with these coastal plumes were believed to be critical in controlling biogeochemical cycling, shaping the light environment, altering available nutrient concentrations, establishing conditions for the spring bloom, and structuring biological communities [*Mortimer*, 1988].

[4] The recurrent turbidity event was first observed in remote sensing data as a highly reflective band near shore [*Mortimer*, 1988]. At that time, Mortimer noted the difficulty in using optical and remote sensing techniques in areas of strong optical gradients and highly variable concentrations of suspended particulate material (SPM), colored dissolved organic matter (CDOM), and chlorophyll such as that observed in coastal areas. Since that time, there has been much debate over the utility of such techniques in dynamic coastal environments. Recent efforts have focused on remote sensing techniques in order to increase sampling resolution to ecologically relevant scales for investigation into the effects of short-term episodic events. As part of the Episodic Events-Great Lakes Experiment (EEGLE), we wanted to quantify the effects of the episodic recurrent turbidity plume on optical parameters, phytoplankton dynamics, remote sensing techniques, and the performance of currently employed coastal algorithms.

2. Methods

2.1. Sampling

[5] Sampling was conducted in the southeastern portion of Lake Michigan (Figure 1) from 24–26 March 1999, 14–15 and 22–24 April 1999, and 18–19 March 2000 onboard the R/V *Laurentian*. Sampling stations were established both inside and outside of the sediment plume along historic transect lines perpendicular to the coast. Vertical profiles of physical and optical parameters were performed at each station and supplemented with discrete water samples that were taken to the laboratory for more in depth analysis.

2.1.1. Optical Measurements

[6] At each station, hydrographic profiles of the water column were measured with a SeaBird CTD. Optical measurements included surface and vertical profiles of both apparent and inherent optical properties. Inherent optical properties (IOPs) were measured with a dual-path absorption and attenuation meter (AC-9; Wetlabs Inc.). The AC-9 measures both absorption and attenuation at 9 wavelengths of light (412, 440, 488, 510, 532, 555, 630, 676, and 715 nm). The AC-9 was factory calibrated between sampling years and calibrated daily using ultra-clean water from a Barnstead E-Pure water purification system. Absorption data were integrated with concurrently collected CTD data and were temperature [*Pegau et al.*, 1997] and scattering (subtraction of a715 from all a channels [*Zaneveld and Kitchen*, 1994]) corrected and binned to 0. 25-m-depth intervals.

[7] Apparent optical properties (AOPs) were collected using a profiling spectral radiometer (Ocean Color Radiometer 200; Satlantic Inc.) and a hyperspectral radiometric buoy (HTSRB; Satlantic Inc.). The OCR-200 measures downwelling irradiance (E_d) and upwelling radiance (L_u) in situ as well as downwelling surface irradiance [$E_d(0^+)$] at 14 wavelengths (305, 324, 339, 380, 406, 412, 443, 490, 510, 555, 619, 665, 670, and 705 nm). The TSRB measures $E_d(0^+)$ and L_u (at 0. 7m) at 123 visible wavelengths. All Satlantic sensors were factory calibrated prior to each sampling year. Collected radiometric data were processed using Satlantic's Prosoft software package according to manufacturer protocols. No dark corrections or self shading corrections were applied to these data. Diffuse attenuation coefficient (K_d) values were calculated as

$$K_d = LN\left(\frac{Ed_2}{Ed_1}\right)\frac{1}{\Delta z}, \tag{1}$$

where E_{d2} is the downwelling irradiance at depth 2, E_{d1} is downwelling irradiance at depth 1, and Δz is the change in depth between these two measurements. Remote sensing reflectance (Rrs) values were calculated using Prosoft as

$$Rrs(0^+,\lambda) = \frac{L_w(0^+,\lambda)}{E_d(0^+,\lambda)}, \tag{2}$$

where L_w is upwelling radiance propagated up through the surface of the water as

$$L_w(0^+,\lambda) = 0.54 L_w(0^-,\lambda). \tag{3}$$

Remote sensing reflectance outputs from Prosoft calculations were subsequently used for calculation of chlorophyll *a* concentrations using an array of remote sensing chlorophyll algorithms (Table 1) [*O'Reilly et al.*, 1998, 2000].

2.1.2. Discrete Sample Measurements

[8] Teflon-coated Niskin bottles, lowered to selected depths, were used to collect water for assessment of

Table 1. Algorithms Used to Calculate Chlorophyll *a* From Remote Sensing Reflectance[a]

Sensor	Equation	R
SeaWiFS/OC2	$C = 10.0^{(0.341-3.001R+2.811R^2-2.041R^3)} - 0.04$	490/555
OCTS/OC4O	$C = 10.0^{(0.405-2.900R+1.690R^2-0.530R^3-1.144R^4)}$	443 > 490 > 520/565
MODIS/OC3M	$C = 10.0^{(0.2830-2.753R+1.457R^2-0.659R^3-1.403R^4)}$	443 > 490/550
CZCS/OC3C	$C = 10.0^{(0.362-4.066R+5.125R^2-2.645R^3-0.597R^4)}$	443 > 520/550
MERIS/OC4E	$C = 10.0^{(0.368-2.814R+1.456R^2+0.768R^3-1.292R^4)}$	443 > 490 > 510/560
SeaWiFS/OC4v4	$C = 10.0^{(0.366-3.067R+1.930R^2+0.649R^3-1.532R^4)}$	443 > 490 > 510/555
SeaWiFS/OC2v4	$C = 10.0^{(0.319-2.336R+0.879R^2-0.135R^3)} - 0.071$	490/555

[a] R is determined as the maximum of the values shown. Sensor algorithms shown are for SeaWiFS (Sea-viewing Wide Field of view Sensor), OCTS (Ocean Color and Temperature Scanner), MODIS (Moderate Resolution Imaging Spectroradiometer), CZCS (Coastal Zone Color Scanner), and MERIS (Medium Resolution Imaging Spectrometer).

phytoplankton photopigments, photosynthesis-irradiance parameters, SPM concentrations, and microphotometry assays. Phytoplankton biomass, as chlorophyll *a*, and phylogenetic group dynamics were characterized using chemotaxonomic pigments derived using High Performance Liquid Chromotography and CHEMTAX as outlined by *Millie et al.* [2002]. Photosynthesis-irradiance parameters were measured as by *Fahnenstiel et al.* [2000]. SPM concentrations were determined gravimetrically after drawing 0.2- to 0.3-L aliquots under low vacuum onto pre-rinsed, tared 47-mm-diameter Poretics 0.4-μm polycarbonate filters. The filters were dried in a dessicator to constant weight. When necessary, SPM concentrations were estimated from AC-9 collected data based upon the relationship established between suspended material concentration and attenuation at 630 nm (Figure 2).

[9] For microphotometry analysis, raw water samples were filtered under low vacuum (<50 mm Hg) onto 1.0-μm Nucleopore filters with GF/A backing filters. When the last 1–2 mL of water was still in the filtering funnel, vacuum pressure was released, and the filter, along with a few drops of water, was transferred to a gelatin slide. It is critical not to filter all of the water, as delicate cells are likely to rupture if some water is not retained on the filter. The back of the filter was gently swiped with a damp cotton swab and then removed from the gelatin slide. One to two drops of a 30% glycerol solution was placed on the transferred samples along with a coverslip. The slide was then immediately frozen by placing it on an aluminum block that had been previously immersed in liquid nitrogen. The frozen slides were placed in a slide box and kept frozen (−20°C) until analysis.

[10] The absorption efficiency factor, Q_a, can be measured on individual cells using a microphotometric technique [*Itturriaga and Siegel*, 1989; *Stephens*, 1995]. This absorption efficiency factor is defined as the ratio of light absorbed by a cell to the light impinging on the cell's geometrical cross section. Microphotometric measurement of Q_a requires direct measurement of spectral transmittance of a cell or particle relative to a blank

$$Q_a(\lambda) = \frac{I_b(\lambda) - I_s(\lambda)}{I_b(\lambda)}, \tag{4}$$

where $I_s(\lambda)$ is the radiant flux or transmittance for the sample, and $I_b(\lambda)$ is the radiant flux or transmittance for the blank. The raw data were smoothed by averaging over five wavelength bins. To correct for any light that might have been lost by scattering, which in our system was likely minimal [*Itturriaga and Siegel*, 1989], the mean Q_a value at 750–760 nm was subtracted from all other measurements.

[11] A Leica DMR HC microscope system equipped with an optic coupler was used for microphotometric measurements. An Ocean Optics, Inc. collimating lens (74-VIS) was used to coupled light from the microscope head to a 400-μm patch silica optical fiber which was interfaced with an Ocean Optics, Inc., miniature spectrometer (S2000) interfaced with a 500-KHz ADC board. The optical configuration provided an effective resolution of approximately 2 nm at full width half maximum (FWHM). The CCD array of the spectrometer consisted of a 2048-element linear detector extending over a wavelength range of 350–1000 nm. Ten scans were averaged for each measurement, and the sampling rate was such that the total scan time was approximately 10 s.

2.2. Solving the Radiative Transfer Equation

[12] In order to evaluate the dynamic response of primary producers to the highly variable in situ light environment, we needed to spectrally characterize the underwater light field under a wide range of conditions. Establishing a solid relationship between the IOPs and AOPs provides confidence that a full set of radiometric parameters can be calculated given in situ measurements of the IOPs. A subsection of our data set (n = 41 profiles) was input into Hydrolight 4.2 (Sequoia Scientific Inc.) to numerically solve the radiative transfer equation for a realistic radiance distribution. Hydrolight requires four basic input parameters: the IOPs of the water body, wind

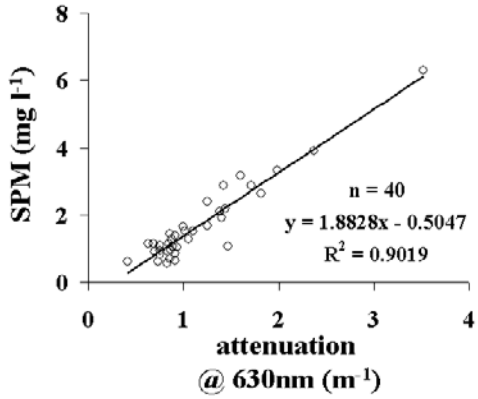

Figure 2. Relationship between attenuation at 630 nm as measured by an AC-9 and suspended particulate material (SPM).

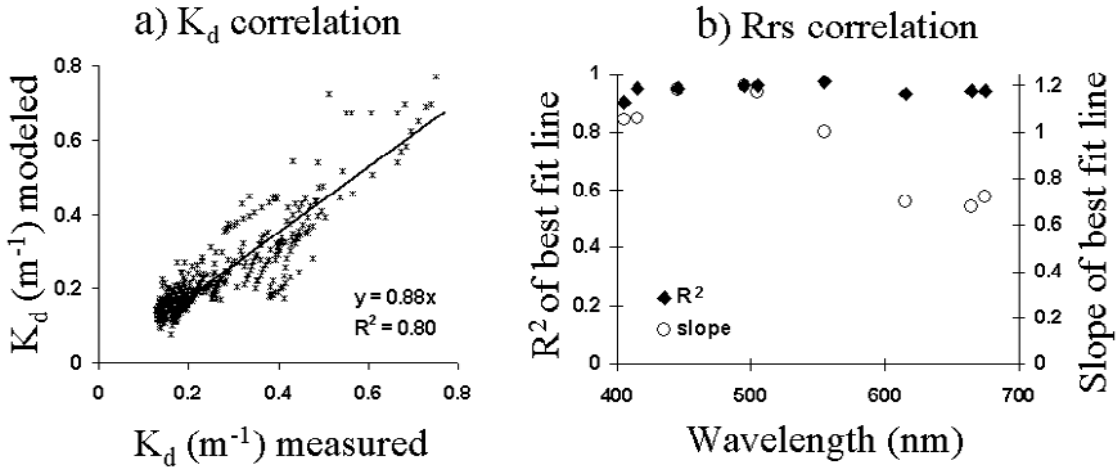

Figure 3. Relationship between measured and modeled apparent optical properties. Measured values are from a Satlantic profiling radiometer and modeled values are from Hydrolight output. (a) Diffuse attenuation coefficient (K_d) for PAR. The solid line is the best fit line with an intercept at the origin. (b) Remote sensing reflectance (Rrs) - R^2 are represented by closed symbols, and the slopes are represented by open symbols.

speed, sky spectral radiance distribution, and water column bottom boundary conditions. In this study we supplied Hydrolight with measured IOPs (a and c) from an AC-9 and measured wind speeds from an anemometer aboard the research vessel. The sky spectral radiance distribution is calculated within Hydrolight via RADTRAN based upon user-supplied date, time of day, location on the globe, and cloud cover at each station. Reflectance of the bottom boundary was set at 20% without spectral dependence for all calculations. In this study, Hydrolight output was obtained solely to determine scalar irradiance values; therefore we wanted to ensure that Hydrolight output closely reflected in situ conditions at the time of sampling. To this end, the backscatter fraction (b_b/b) was optimized at each individual station to minimize the difference between the output and measured values and was input as a Fournier-Fourand (FF) phase function. In the absence of a measured particle phase function, the FF is an acceptable replacement as the exact shape of the phase function is not as critical as the magnitude of the backscatter ratio for calculations of the AOPs [*Mobley et al.*, 2002].

[13] To validate our results from Hydrolight, modeled values were compared to concurrently measured AOPs at 41 stations in our sampling area over the course of 2 years in the spring and summer. These stations encompassed a wide variety of optical and physical environments. K_d and Rrs values were used for the comparisons as they are not extremely sensitive to the geometric distribution of the light field. To correlate K_d, we incorporated 435 data points over spatial and temporal gradients and directly compared the Hydrolight output with measured values (Figure 3a). The correlation was strong with a slope of 0.88 indicating that modeled values were slightly underestimating measured K_d values. Rrs correlations were also strong (average R^2 = 0.94) although spectrally dependent (Figure 3b). The slope was very close to 1.0 at lower wavelengths and dropped off toward the red wavelengths (slope range is 0.68–1.2). This is not surprising, as the magnitude of the Rrs signal is much lower in the red wavelengths of light; therefore part of the error in this portion of the spectrum is a signal to noise problem.

[14] Hydrolight output was used to quantify the amount of light available to phytoplankton. Phytoplankton populations are able to use light from all directions for photosynthesis. This light field is represented by the scalar irradiance (E_o). E_o is the integral of the radiance over all angles around a point; this differs from the downwelling irradiance (E_d), which is the traditionally measured irradiance term. E_d accounts only for light propagating in the downward direction and proportionally weights the contribution of radiation at different incidence angles. The E_o output from Hydrolight calculations allowed us to use this E_o term, which we were unable to measure, to examine light utilization by phytoplankton. E_o values were used to calculate the scalar diffuse attenuation coefficient (K_o),

$$K_o = LN\left(\frac{Eo_2}{Eo_1}\right)\frac{1}{\Delta z}, \tag{5}$$

the scalar optical depth (ζ_o),

$$\zeta_o = K_o z, \tag{6}$$

and the average cosine,

$$\overline{\mu} = \frac{E_d - E_u}{E_o}, \tag{7}$$

where E_u is the upwelling irradiance.

3. Results

3.1. Optical Dynamics

[15] The springtime recurrent turbidity plume in Lake Michigan strongly impacted the optical environment in the southern portion of the lake. The plume can easily be

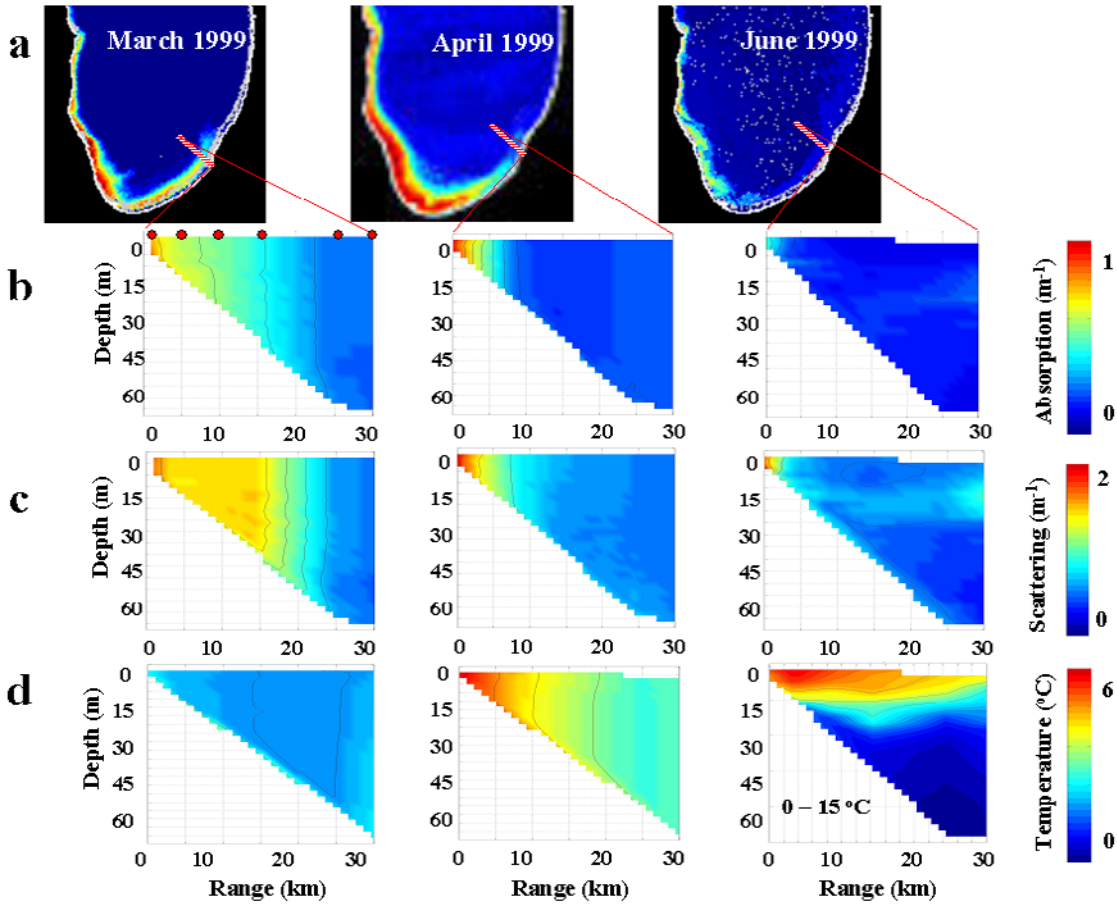

Figure 4. Temporal evolution of the southern Lake Michigan recurrent turbidity plume. (a) AVHRR remote sensing reflectance and (b) absorption, (c) scattering, and (d) temperature along the transect line shown extending 30 km offshore St. Joseph, Michigan. Red circles in Figure 4b represent station locations of the six sampling stations (stations were located approximately 2, 5, 10, 16, 26, and 30 km from shore). Note the change in scale for the temperature plot associated with June 1999.

observed in remote sensing reflectance imagery during the spring months (Figure 4a). The spatial extent of the plume can be seen in March 1999, followed by confinement to the coastline in April, and then dissipation in the summer months with thermal stratification (Figure 4). The three major optical zones along a transect line in April 1999 extending 32 km offshore St. Joseph, Michigan, through the sediment plume area, can readily be observed in collected data. The optical gradients in this area were large over short distances, reflecting the interaction of the turbidity plume and outflow from the St. Joseph River. The three distinct water types along this transect line included an onshore river/plume region that extended to roughly 10 km offshore, plume-dominated water that extended approximately 10 to 20 km offshore, and offshore stations farther than 20 km. Data collected along this transect line in April of 1999 were representative of conditions during the spring of all sampling years for the duration of the sediment plume and were used as a case example during this study.

[16] Nearshore stations were strongly influenced by both the sediment plume and the outflow from the St. Joseph River. Although absorption and scattering were both increased at nearshore stations, spectral changes in the optical signal were controlled by absorption. Concentrations of highly absorbing CDOM and chlorophyll *a* were increased in onshore stations relative to offshore areas. CDOM absorbs light mostly in the blue wavelengths, which was apparent as an increase in the absorption spectra in the blue wavelengths (Figure 5a). These high nearshore CDOM concentrations were probably due to both river outflow and in situ production. Chlorophyll *a* concentrations at onshore stations were relatively high, and diatoms dominated the phytoplankton community, adding to the high blue light absorption values (Figures 6d–6f). The effects of in-water constituents were also apparent in the Rrs spectra. Onshore stations had a proportional decrease in Rrs in the 400- to 500-nm region relative to stations farther offshore due to absorption of light by both CDOM and chlorophyll *a* at these wavelengths. A peak in Rrs due to chlorophyll fluorescence at 676 nm is also evident (Figure 6b, red line). The available light field at the 1% light level was predominately green and red as all of the shorter wavelengths of light were absorbed in the water column (Figure 6c).

[17] Moving offshore into waters impacted less by the river, the effects of the sediment plume became more apparent. Absorption values decreased relative to onshore stations while scattering stayed high, resulting in a signif-

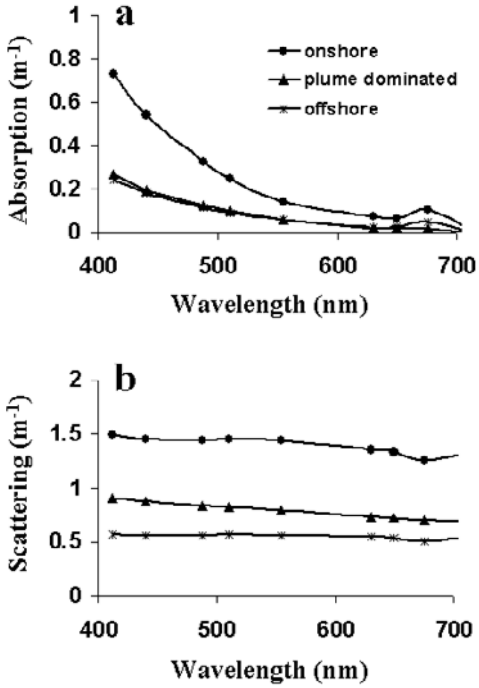

Figure 5. Spectral (a) absorption and (b) scattering coefficients at three stations along an April 1999 cross-shelf transect offshore St. Joseph, Michigan, measured with and calculated from an AC-9. Stations are located onshore (circles, 2 km offshore), in plume-dominated waters (triangles, 10 km offshore), and offshore (stars, 30 km offshore).

icant increase in measured b/a ratios (Figure 6a). This high scattering-to-absorption ratio was used as the primary optical signature of the sediment plume. The proportional decrease in absorption and increase in scattering was reflected in higher Rrs signals as more light was scattered up through the water column (Figure 6b, green line). Chlorophyll values decreased in plume-dominated stations, and the composition of the phytoplankton community began to change (Figures 6d–6f). Farther offshore, the optical signature was dominated by phytoplankton absorption. Both absorption and scattering were low relative to onshore waters, and Rrs spectra were comparatively low and spectrally flat (Figure 6b, blue line). Available light at the 1% light level was mostly blue-green, and the phytoplankton community became dominated by cryptophyte algae in these offshore waters (Figures 6c and 6e).

[18] The changes in the concentrations of optically active constituents altered the light climate of the different water types. The high blue absorption at onshore stations resulted in the selective removal of blue wavelengths and a red shift of the available light field, while offshore stations had proportionally more blue and green light (Figure 6c). In addition to these spectral changes in light quality, the quantity of available light at depth was decreased in onshore stations. The relationship between scalar optical depth and physical depth was steeper at onshore stations than in plume-dominated and offshore waters (Figure 7a). A deeper optical depth corresponding to the same physical depth indicates that onshore waters were more attenuating than offshore waters. Additionally, the scattering/absorption ratio was higher in plume-dominated stations as compared to both onshore and offshore waters, resulting in a change in the diffusivity of the underwater light. The average cosine provides a simple description of the angular radiance distribution of the underwater light field. Average cosine values range from 0 for isotropic light fields to 1 in a collimated beam of light; a lower average cosine value indicates a more diffuse light field. In regions affected by the turbidity plume, the increased scattering resulted in a lower average cosine (Figure 7b). The average cosine was lowest in areas most optically impacted by the plume and highest in clearer, offshore waters.

3.2. Biological Dynamics

[19] Phytoplankton physiology and community composition were notably impacted by both seasonal changes in the light environment and the optical gradients observed in the spring. The phytoplankton photosynthetic physiology reflected the seasonal variations in the light climate. The irradiance levels corresponding to the photoacclimation parameter (E_k) and the light-saturated photosynthetic rate ($P^b_{\max}$) were relatively constant at 77 (±16) μmol photons m^{-2} s^{-1} and 0. 61 (±0.28) μg C μg chl^{-1} h^{-1}, respectively, both in the spring months and during the summer in deeper waters (Figure 8). E_k values were not dependent on in situ E_o at the time of sample collection in these data. However, summer surface samples, which were collected at a shallower scalar optical depth (samples collected above the thermocline), were dependent on in situ E_o values. As relative E_o at the time of sample collection increased due to the change in season and the shallowing of the mixed layer depth with the onset of stratification, the associated E_k and $P^b_{\max}$ values increased. These populations were consistently exposed to higher light levels in surface waters and acclimated to their growth conditions. There was no correlation between SPM concentrations and E_k for any of the samples collected; thus changes in the photoacclimation parameter were not associated with the sediment plume (Figure 8).

[20] The distribution of total chlorophyll and the composition of phytoplankton communities also varied as the optical environment changed during the spring sampling period. Diatoms consistently comprised a higher proportion of chlorophyll *a* onshore and in surface waters, while cryptophytes comprised a higher proportion offshore and in deeper waters (Figures 6d–6e). This resulted in a strong inverse relationship between diatom and cryptophyte abundances (Figure 9).

4. Discussion

[21] The springtime recurrent turbidity plume observed in southern Lake Michigan established a strong gradient ideal for assessing the utility of optical techniques in coastal waters. The location and extent of the plume could be determined through both remote sensing and in situ sampling techniques (Figures 4 and 6). The plume region, delineated by high reflectance values, extended approximately 20 km offshore for much of the EEGLE study. As seen in previous years, the sediment plume began in the early spring and lasted until early summer.

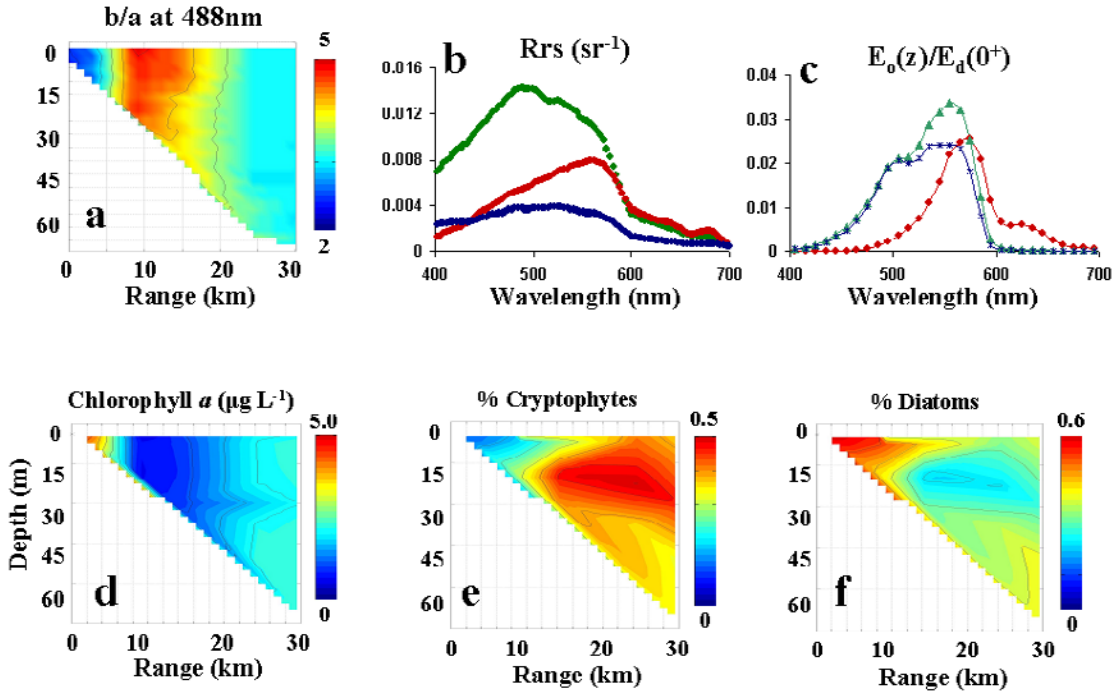

Figure 6. Optical and biological properties associated with an April 1999 cross-shelf transect offshore St. Joseph, Michigan. (a) Scattering/absorption ratio at 488 nm, (b) remote sensing reflectance at an onshore station (red line, 2 km offshore), a plume-dominated station (green line, 10 km offshore), and an offshore station (blue line, 30 km offshore), (c) fraction of available light at the 1% light level, as E_o at depth normalized to E_d at the surface (station colors as in Figure 6b), (d) HPLC measured chlorophyll *a* concentrations, (e) percent of total chlorophyll *a* associated with cryptophytes, and (f) percent of total chlorophyll *a* associated with diatoms. Sampling locations are as in Figure 4.

[22] The sharp optical gradients encountered in the sampling area allowed the impact of variable in-water constituents on remote sensing reflectance to be characterized. Remote sensing reflectance offshore of the St. Joseph River showed the characteristic low blue reflectance due to high concentrations of CDOM and chlorophyll *a* that is common in areas offshore of large rivers (Figure 6b). The St Joseph River drains a watershed area of 694,000 acres mainly through agricultural areas of Indiana and is considered a significant source of dissolved organic carbon [*Mortimer*, 1988]. Conversely, in offshore waters, reflectance was greatest in the blue wavelengths as absorption by phytoplankton and water dominated light attenuation. The sediment plume was characterized by high blue and green Rrs

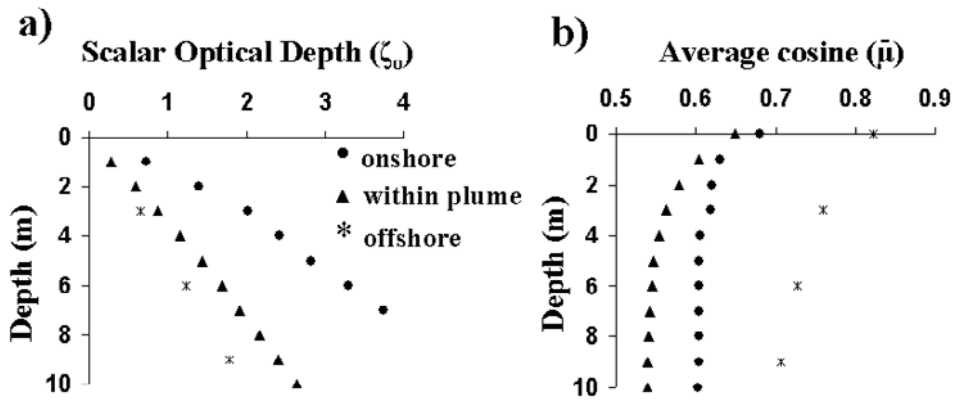

Figure 7. Vertical light properties at April 1999 sampling stations onshore (circles, 2 km offshore), in plume-dominated waters (triangles, 10 km offshore), and offshore (stars, 30 km offshore). (a) Scalar optical depth (ζ_o) for PAR and (b) average cosine (μ) at depth for PAR. A steeper scalar optical depth represents clearer waters (slope values: onshore = 2.12, plume dominated = 3.84, and offshore = 5.33). A lower average cosine indicates a more diffuse light field.

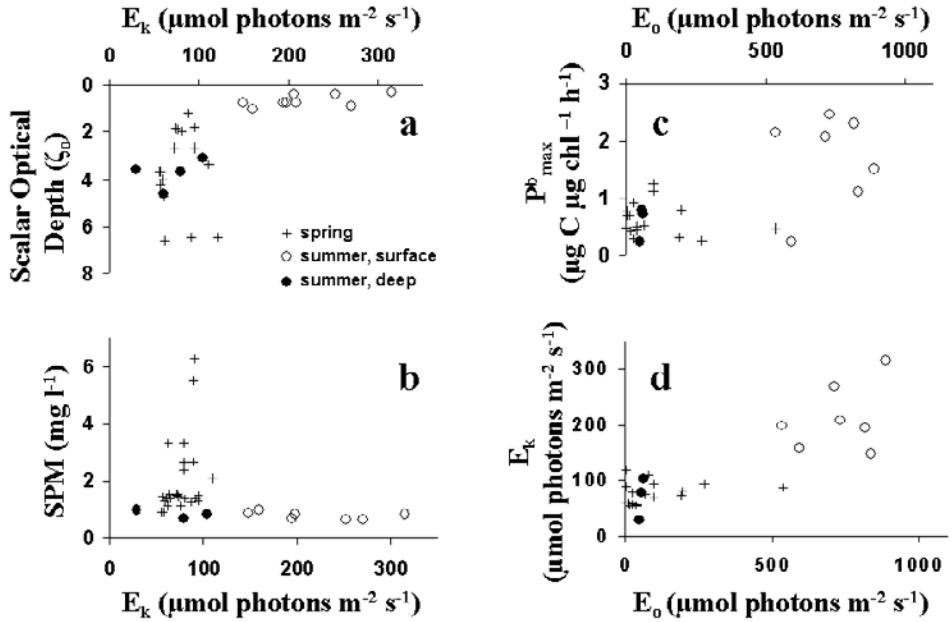

Figure 8. Seasonal variability in physiological parameters. (a) Variability in E_k with scalar optical depth, (b) relationship between E_k and suspended particulate material, (c) relationship between $P^b_{\max}$ and in situ E_o at the time of sample collection, and (d) relationship between E_k and in situ E_o at the time of sample collection. During the spring mixed months E_k and $P^b_{\max}$ values were relatively constant at 77 (±16) µmol photons m^{-2} s^{-1} and 0.61 (±0.27) µg C µg chl^{-1} h^{-1}, respectively, and did not depend on available irradiance (E_o) at the sampling depth (plus symbols). During the summer, stratified months, E_k and $P^b_{\max}$ remained low in bottom waters below the thermocline (solid circles), but were much higher in surface waters (open circles). SPM values were much higher during the spring turbidity event (2.01 ± 1.33 mg L^{-1}) compared to summer time values (0.79 ± 0.12 mg L^{-1}), but there was no significant relationship between measured SPM values and E_k.

values due to the reflective materials in Lake Michigan which are eroded from either alongshore bluffs or shallow water glacial deposits; the sediment composition in the southeastern part of the lake is dominated by these silts and fine sands [*Fahnenstiel and Scavia*, 1987; *Eadie et al.*, 1996; *Barbiero and Tuchman*, 2000]. This reflective material effectively scatters all of the available light and absorbs very little, resulting in high Rrs values.

[23] It was initially believed that the high sediment concentrations associated with the turbidity plume would significantly affect the magnitude of the underwater light field resulting in light-limited phytoplankton populations leading to a decrease in primary productivity [*Millie et al.*, 2002]. However, in plume-dominated stations, the incident integrated flux of light was not significantly different than clearer, non-plume offshore waters which had deep mixed layer depths (Figure 6c). The increased concentration of particles in the sediment plume resulted in increased scattering (Figure 5), which led to a more diffuse light field (Figure 7b). This scattered light is simply redirected and may still be available for absorption by photosynthetic organisms.

[24] Measured photosynthesis irradiance parameters suggested that phytoplankton populations in plume waters were not significantly more low-light acclimated than phytoplankton in offshore stations (Figure 8). E_k values were fairly uniform throughout the spring bloom and plume events; furthermore, the E_k values were not significantly correlated with either suspended particulate material concentrations or light attenuation measurements. Thus there was no observed gradient in phytoplankton photoacclimation between plume and non-plume stations in the spring.

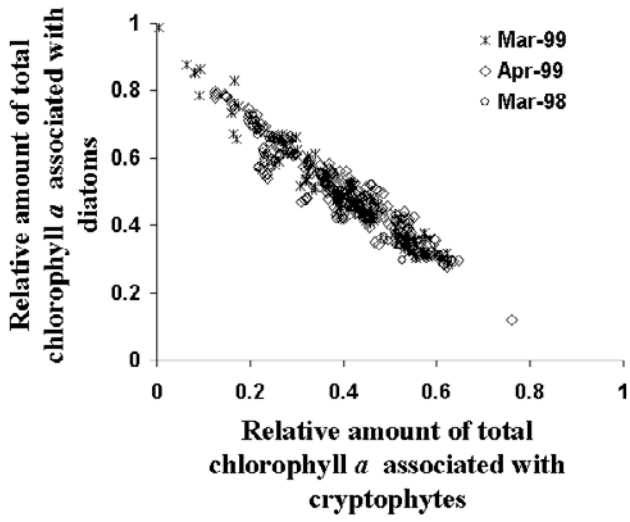

Figure 9. Percentage of total chlorophyll *a* associated with cryptophytes versus percentage of total chlorophyll *a* associated with diatoms from CHEMTAX output for all available data from 1998 and 1999.

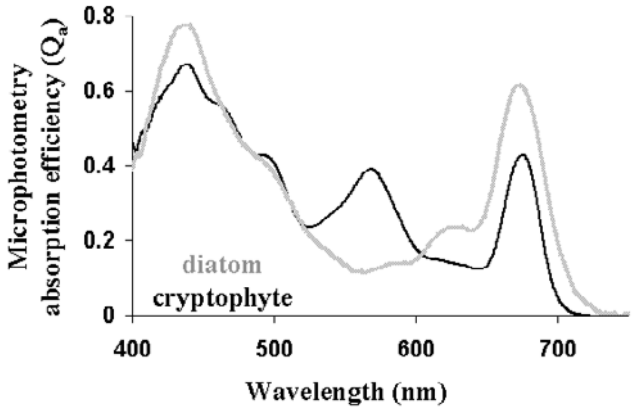

Figure 10. Microphotometry absorption efficiency (Q_a) for a representative diatom (*Melosira islandica*, shaded line) and cryptophyte (*Rhodomonas minuta*, black line) collected offshore St. Joseph, Michigan.

However, the significant increase in E_k and $P^b_{\max}$ with summer stratification indicated that these populations were capable of photoacclimation; springtime populations were low-light acclimated compared to summer populations. This low-light acclimation reflected the deep mixing of springtime populations.

[25] The actual light field available to phytoplankton cells is the depth-integrated light field as they vertically cycle through the water column [*Cullen and Lewis*, 1988]. Under these conditions, cells may photoacclimate to the average light intensity encountered over time. The increase in light attenuation in the plume was balanced offshore where the mixed layer depth was deeper so that phytoplankton populations in these two areas had similar total amounts of light available to them over time. However, the photoacclimation observed in spring populations changed as stratification developed in the summer, which is consistent with the historical model for Lake Michigan phytoplankton [*Fahnenstiel et al.*, 1989]. Summer samples showed a distinct difference in photoacclimation between deep water and surface stations (Figure 8). Surface samples were more acclimated to the incident light field at the time of sample collection, whereas photoacclimation parameters for deep water samples collected below the thermocline were independent of the incident light field (Figures 8c and 8d). Deep water samples collected below the thermocline (thermocline at approximately 20 m; Figure 4d) and spring samples were being mixed over a wide vertical range of varying light intensity. The rate of mixing was most likely faster than the rate of photoacclimation, and these samples were unable to acclimate to the ever-changing light intensity.

[26] Although the intensity of light in both plume-dominated and offshore stations in spring was similar when averaged over the depth of the water column, the average light field for a deep water station was spectrally different than a shallower station. Deep-water stations had a distinct spectral shift in available light, with green light dominating at depth. This greening of the water altered the competitive ability of the two main phytoplankton classes encountered in Lake Michigan. The observed shift in the phytoplankton community from diatoms onshore to cryptophytes offshore was controlled in part by the spectral shift in the available light field. Although the absorption efficiencies for a representative diatom (*Melosira islandica*) and cryptophyte (*Rhodomonas lens*) were equal when integrated under PAR, they were distinctly spectrally different (Figure 10). *M. islandica* and *R. lens* are prevalent species in Lake Michigan that significantly contribute to total phytoplankton biomass [*Holland*, 1969; *Danforth and Ginsburg*, 1980; *Makarewicz et al.*, 1994]. The primary photosynthetic pigments for diatoms are chlorophyll and fucoxanthin, which absorb maximally in the blue and red wavelengths of light, while the cryptophytes primarily utilize phycobilin pigments, which have an absorption maximum in the green wavelengths. The potential for growth for photosynthetic organisms is dependent upon their ability to absorb the spectra of light that is available.

[27] The incoming irradiance at the sea surface is spectrally flat (Figure 11a, shaded area). In this white light environment the total absorption by phytoplankton is independent of the spectral nature of the light field. Potential absorption for *M. islandica* and *R. lens* was calculated based upon their measured absorption efficiencies and the available irradiance at both the surface and for the average light field throughout the mixed layer depth at an offshore station (Figure 11). In surface waters with a spectrally unrestricted light field, potential absorption efficiencies for *M. islandica* and *R. lens* were approximately equal when integrated under

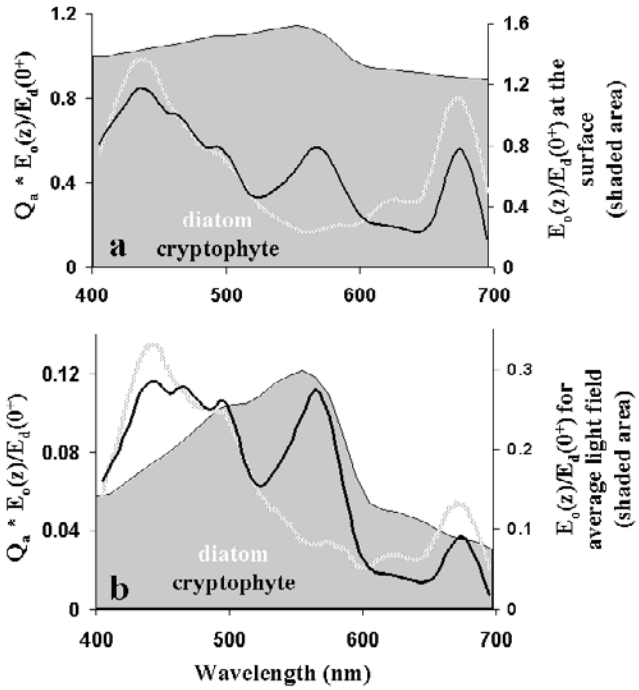

Figure 11. Product of the absorption efficiency (Q_a) for a representative diatom (shaded line) and cryptophyte (black line) and the scalar irradiance (E_o), normalized to the downwelling irradiance at the surface. (a) Scalar irradiance at the surface $E_o(0^-)$ and (b) scalar irradiance for the average light field experienced by a phytoplankton cell over the mixed layer depth assuming total mixing of the water column. Superimposed is the available light field in light shading.

Table 2. Correlation Results for the Calculation of Chlorophyll From Remote Sensing Reflectance Measurements[a]

Sensor/Algorithm	Slope, All Stations	R^2, All Stations	Slope, Non-Cryptophyte-Dominated Stations	R^2, Non-Cryptophyte-Dominated Stations
SeaWiFS/OC2	0.81	0.66	1.04	0.95
OCTS/OC4O	0.54	0.81	0.6	0.89
MODIS/OC3M	0.6	0.77	0.7	0.89
CZCS/OC3C	0.57	0.76	0.65	0.88
MERIS/OC4E	0.59	0.79	0.62	0.87
SeaWiFS/OC4v4	0.65	0.68	0.73	0.83
SeaWiFS/OC2v4	0.68	0.69	0.78	0.83

[a]Slope and R^2 for the linear correlation between measured and calculated chlorophyll is shown (as in Figure 12) for all stations and for a subset of stations where the phytoplankton community composition is not dominated by cryptophytes (less than 40% of total chlorophyll *a* attributed to cryptophytes). All of the algorithms perform better in areas that were not significantly influenced by cryptophyte absorption.

the visible light curve (Figure 11a). Under these conditions, all phytoplankton groups are at their maximum potential for light absorption. Assuming that the isothermal water columns were completely vertically mixed during the spring months (Figure 4d), an average light field was computed based upon the spectral light availability in the mixed layer depth. This average light field is spectrally skewed as the blue and red wavelengths of light are selectively removed leaving mostly green light (Figure 11b). Although the potential absorption for both species was equal at the surface, the cryptophytes had a higher potential for absorption in the average mixed layer depth light field. The chlorophyll and fucoxanthin pigments of the diatom were less effective than the cryptophyte's phycobilin pigments as the light field became more restricted to the green wavelengths of light. Given the spectral quality of light at depth in the lake, the cryptophytes were better suited to utilize the available irradiance. This spectral selection for cryptophytes may explain the offshore distribution observed in phytoplankton populations. This is consistent with the idea that absorption of green light by phycobilins in cyanobacteria may allow them to be superior competitors at depth in spectrally skewed light fields [*Huisman et al.*, 1999].

[28] Additionally, cryptophytes may be able to supplement their nutritional needs heterotrophically at low light levels [*Faust and Gantt*, 1973; *Lewitus et al.*, 1991] and are efficient swimmers capable of crossing ecologically relevant physical boundaries [*Jones*, 1988]. In nature, the ability to supplement photosynthetic growth with the uptake of organic nutrients and the vertical migrations

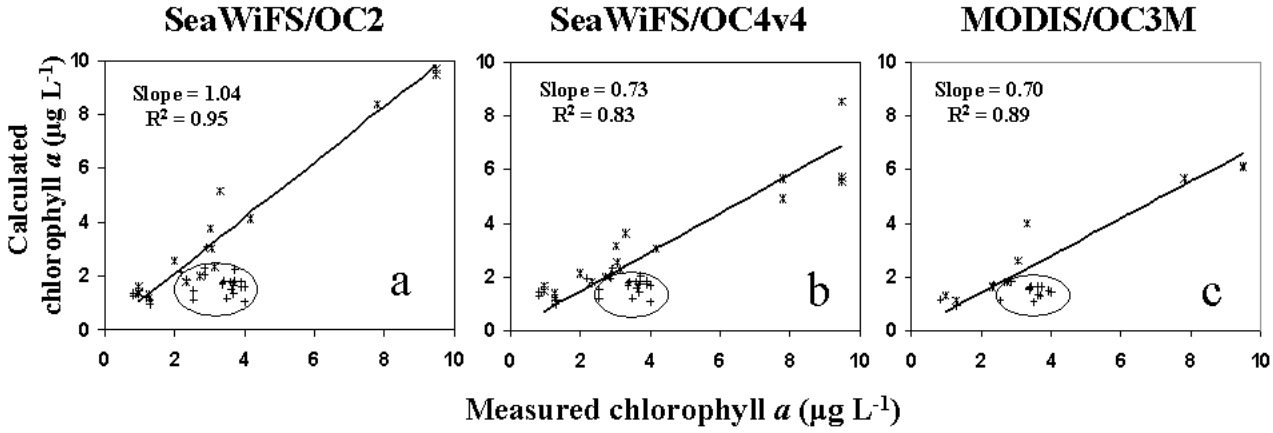

Figure 12. Relationship between measured chlorophyll *a* (HPLC) and calculated chlorophyll *a* from three currently used ocean color algorithms. (a) SeaWiFS OC2, (b) SeaWiFS OC4v4, and (c) MODIS OC3M. The relationship is strong until the optical signal is affected by cryptophyte absorption. The circled stations are those where cryptophytes make up 40% or more of the total chlorophyll *a*. The solid line is the best fit line through data not including cryptophyte-dominated stations; reported slope and R^2 values are for this best fit line (also see Table 2). To verify the significance of this difference, a series of t-tests were run to compare measured and calculated chlorophyll values for all algorithms tested for the same subset of stations where the phytoplankton community composition is not dominated by cryptophytes (n = 18) and also for the remaining stations which are dominated by cryptophytes (n = 25). *P* values for a comparison between chlorophyll calculated at stations dominated by cryptophytes and chlorophyll measured values were all <0.0001. These results show that there is a statistically significant difference between measured and calculated chlorophyll concentrations in areas that were dominated by cryptophytes.

observed in cryptophytes leads to increases in their growth rates [*Ojala et al.*, 1996]. These strategies may also play a role in the cryptophyte's enhanced growth at depth relative to diatoms.

[29] The observed shifts in phytoplankton community composition impacted remote sensing reflectance and thus ocean color algorithms. There was a strong correlation between measured and calculated chlorophyll concentration at most stations (Table 2). However, the absorption of green light by cryptophytes selectively removes these wavelengths from the light field. Chlorophyll algorithms utilize Rrs band ratios, which include 550-, 555-, 560-, and 565-nm green light reflectance. These ratios assume case 1 waters where the in situ absorption and water leaving radiance (L_w) signal in the blue wavelengths is dominated by chlorophyll absorption while L_w in the green wavelengths is insensitive to chlorophyll concentrations [*Gordon and Morel*, 1983]. However, in Lake Michigan, cryptophyte absorption selectively removed the green light from the reflectance signal. Areas that were not dominated by cryptophytes (those with less than 40% of total chlorophyll contributed by cryptophytes) showed good agreement between measured and satellite estimated chlorophyll concentrations (Figure 12; Table 2). In regions with high concentrations of phycobilin containing algae, remotely estimated chlorophyll concentrations were underestimated by an average of 45% for all algorithms tested. Thus, contrary to previous beliefs, the sediment plume had little affect on the utility of ocean color remote sensing efforts. The critical parameter impacting the performance of ocean color algorithms in this area was the community composition of phytoplankton.

5. Summary and Conclusions

[30] Our results illustrate the minimal effect of the sediment plume on the quantity of available light for phytoplankton populations. There was no significant change in the photosynthetic characteristics between plume and non-plume populations. The phytoplankton plume populations were not significantly low-light acclimated compared to populations in clearer waters offshore. The composition of phytoplankton communities may have been impacted by the spectral quality of light, which was a function of the mixed layer depth and the in-water constituents. In the deep, well-mixed water columns, the average spectral light field was increasingly spectrally skewed which is common in freshwater systems [*Kirk*, 1994]. As the average light distribution becomes spectrally restricted, the ability of phytoplankton to absorb light is directly related to the spectral nature of their light-harvesting capabilities. In Lake Michigan this may account for the distribution of diatoms nearshore and cryptophytes offshore where phycobilin pigments efficiently absorb the available green light. Surprisingly, variability in SPM concentrations caused by the spring resuspension event had no effect on estimating chlorophyll using current satellite algorithms. However, changes in the phytoplankton community structure did impact chlorophyll remote sensing algorithms such that these algorithms did not perform well in offshore areas dominated by phycobilin containing cryptophyte algae. This suggests that currently employed reflectance algorithms may be compromised in regions of highly variable phytoplankton community composition.

[31] **Acknowledgments.** Many thanks to Larry Boihem, Kimberly Kelly, Augie Kutlewski, Merritt Tuel, Rich Stone, and the captain and crew of the R/V *Laurentian*. Additionally, we would like to thank Emmanuel Boss, John Klinck, and three anonymous reviewers for their helpful comments. Funding was provided by NSF (OCE-9727341 and OCE-9727342) and NOAA through the CoOP Great Lakes Initiative and by ONR's Hyperspectral Coastal Ocean Dynamics Experiment (HyCODE, N0014-99-0196).

References

Barbiero, R., and M. Tuchman (2000), Results from the Great Lakes National Program Office's Biological Open Water Surveillance Program of the Laurentian Great Lakes for 1998, report, U.S. EPA Great Lakes Program, Chicago, Ill.

Beletsky, D., and D. Schwab (2001), Modeling circulation and thermal structure in Lake Michigan: Annual cycle and interannual variability, *J. Geophys. Res.*, *106*(C9), 19,745–19,771.

Cullen, J., and M. Lewis (1988), The kinetics of algal photoadaptation in the context of vertical mixing, *J. Plankton Res.*, *10*, 1039–1063.

Danforth, W., and W. Ginsburg (1980), Recent changes in the phytoplankton of Lake Michigan near Chicago, *J. Great Lakes Res.*, *6*(4), 307–314.

Eadie, B., R. L. Chambers, W. S. Gardner, and G. I. Bell (1984), Sediment trap studies in Lake Michigan: Resuspension and chemical fluxes in the southern basin, *J. Great Lakes Res.*, *10*(3), 307–321.

Eadie, B., et al. (1996), Development of recurrent coastal plume in Lake Michigan observed for first time, *EOS*, *77*(35), 337–338.

Fahnenstiel, G. L., and D. Scavia (1987), Dynamics of Lake Michigan phytoplankton: The deep chlorophyll layer, *J. Great Lakes Res.*, *13*(3), 285–295.

Fahnenstiel, G. L., J. F. Chandler, H. J. Carrick, and D. Scavia (1989), Photosynthetic characteristics of phytoplankton communities in Lakes Huron and Michigan: P-I parameters and end-products, *J. Great Lakes Res.*, *15*(3), 394–407.

Fahnenstiel, G. L., R. A. Stone, M. J. McCormick, C. L. Schelske, and S. E. Lohrenz (2000), Spring isothermal mixing in the Great Lakes: Evidence of nutrient limitation and nutrient-light interactions in a suboptimal light environment, *Can. J. Fish. Aquat. Sci.*, *57*, 1901–1910.

Faust, M., and E. Gantt (1973), Effect of light intensity and glycerol on the growth, pigment composition, and ultrastructure of *Chroomonas* sp., *J. Phycol.*, *9*, 489–495.

Gordon, H., and A. Morel (1983), *Remote Assessment of Ocean Color for Interpretation of Satellite Visible Imagery*, Springer-Verlag, New York.

Hawley, N. (1991), Preliminary observations of sediment erosion from a bottom resting flume, *J. Great Lakes Res.*, *17*(3), 361–367.

Holland, R. (1969), Seasonal fluctuations of Lake Michigan diatoms, *Limnol. Oceanogr.*, *14*, 423–436.

Huisman, J., P. van Oostveen, and F. J. Weissing (1999), Species dynamics in phytoplankton blooms: Incomplete mixing and competition for light, *Am. Nat.*, *154*(1), 46–68.

Itturriaga, R., and D. Siegel (1989), Microphotometric characterization of phytoplankton and detrital absorption properties in the Sargasso Sea, *Limnol. Oceanogr.*, *34*(8), 1706–1726.

Jones, R. (1988), Vertical distribution and diel migration of flagellated phytoplankton in a small humic lake, *Hydrobiologia*, *161*, 75–87.

Kirk, J. (1994), *Light and Photosynthesis in Aquatic Ecosystems*, Cambridge Univ. Press, New York.

Lee, C., and N. Hawley (1998), The response of suspended particulate material to upwelling and downwelling events in southern Lake Michigan, *J. Sediment. Res.*, *68*(5), 819–831.

Lewitus, A. J., D. A. Caron, and K. R. Miller (1991), Effects of light and glycerol on the organization of the organization of the photosynthetic apparatus in the facultative heterotroph *Pyrenomonas salina* (Cryptophyceae), *J. Phycol.*, *27*, 578–587.

Lou, J., D. Schwab, D. Beletsky, and N. Hawley (2000), A model of sediment resuspension and transport dynamics in southern Lake Michigan, *J. Geophys. Res.*, *105*, 6591–6610.

Makarewicz, J., T. Lewis, and P. Bertram (1994), Epilimnetic phytoplankton and zooplankton biomass and species composition in Lake Michigan, 1983 to 1992, U.S. Environ. Prot. Agency, Chicago, Ill.

Millie, D., G. Fahnenstiel, H. J. Carrick, S. E. Lohrenz, and O. M. E. Schofield (2002), Phytoplankton pigments in coastal Lake Michigan: Distributions during the spring isothermal period and relation with episodic sediment resuspension, *J. Phycol.*, *38*, 639–648.

Mobley, C. D., L. K. Sundman, and E. Boss (2002), Phase function effects on oceanic light fields, *Appl. Opt.*, *41*(6), 1035–1050.

Mortimer, C. (1988), Discoveries and testable hypotheses arising from Coastal Zone Color Scanner imagery of southern Lake Michigan, *Limnol. Oceanogr.*, *33*(2), 203–226.

Ojala, A., S. Heaney, L. Arvola, and F. Barbosa (1996), Growth of migrating and non-migrating cryptophytes in thermally and chemically stratified experimental columns, *Freshwater Biol.*, *35*, 599–608.

O'Reilly, J., S. Maritorena, B. G. Mitchell, D. A. Siegel, K. L. Carder, S. A. Garver, M. Kahru, and C. McClain (1998), Ocean color algorithms for SeaWiFS, *J. Geophys. Res.*, *103*, 24,937–24,953.

O'Reilly, J. E., et al. (2000), SeaWiFS postlaunch technical report series, in *SeaWiFS Postlaunch Calibration and Validation Analyses*, *NASA Tech. Memo.*, *11*(3).

Pegau, W., D. Gray, and J. R. V. Zaneveld (1997), Absorption and attenuation of visible and near-infrared light in water: Dependence on temperature and salinity, *Appl. Opt.*, *36*(24), 6035–6046.

Stephens, F. (1995), Variability of spectral absorption efficiency within living cells of *Pyrocystis lunula* (Dynophyta), *Mar. Biol.*, *122*, 325–331.

Zaneveld, J., and J. Kitchen (1994), The scattering error correction of reflecting tube absorption meters, *Proc. SPIE Intl. Soc. Opt. Eng.*, *2258*, 44–55.

T. Bergmann, School of Marine Sciences, University of Maine, Orono, ME 04473, USA. (bergmann@maine.edu)

G. Fahnenstiel, Great Lakes Environmental Research Laboratory, NOAA, 1431 Beach Street, Muskegon, MI 49441, USA. (fahnenstiel@glerl.noaa.gov)

S. Lohrenz, Department of Marine Science, University of Southern Mississippi, Stennis Space Center, MS 39529, USA. (steven.lohrenz@usm.edu)

D. Millie, Florida Marine Research Institute, FWCC & Florida Institute of Oceanography, 100 Eighth Avenue, S.E., Saint Petersburg, FL 33701, USA. (david.millie@fwc.state.fl.us)

O. Schofield, Coastal Ocean Observation Lab, Institute of Marine and Coastal Sciences, Rutgers University, New Brunswick, NJ 08901, USA. (oscar@imcs.rutgers.edu)